JSEE Vol. 22, No. 1, 2020 DOI:10.48303/jsee.2020.246184

Pore Pressure Build-Up in Aggregate-Clay Mixtures under Cyclic Loading

Ali Shafiee[1], Javad Jalili[2*], Hamid R. Tavakoli[3], and Mohammad K. Jafari[4]

1. Assistant Professor, California State Polytechnic University, Pomona, Civil Engineering Department, College of Engineering, CA, USA
2. Assistant Professor, Geotechnical Research Center, International Institute of Earthquake Engineering and Seismology(IIEES), Tehran, Iran,
*Corresponding Author; email: jalili@iiees.ac.ir
3. Associate Professor, Civil Engineering Department, Babol Noshirvani University of Technology, Babol, Iran
4. Professor, Earthquake Risk Management Research Center, International Institute of Earthquake Engineering and Seismology (IIEES), Tehran, Iran

Received: 14/07/2020
Accepted: 09/05/2021

ABSTRACT

Undrained behavior of aggregate-clay mixtures in its natural or compacted state, which is used as the core of embankment dams or liner of waste disposal systems, has great importance for geotechnical engineers. Previous studies have shown that excess pore water pressure plays an important role when dealing with cyclic/ dynamic behavior of aggregate-clay mixtures. An extensive testing program was conducted on compacted sand-clay mixtures to investigate effects of aggregates on the cyclic behavior of the mixtures under strain- and stress-controlled cyclic loads utilizing triaxial and torsional shear equipment. Clay content was varied from 100 to 40% by volume in tested specimens. Isotropically and anisotropically consolidated specimens were tested under vertical effective stresses of 100 and 500 kPa. The aim of the various loading conditions and numerous experiments was to investigate cyclic pore pressure build-up in the mixtures, and developing a pore pressure model based on dissipated energy. The main advantage of the model is that it can capture opposite trend of pore pressure build-up with aggregate content in strain-, and stress-controlled loading. The model is then verified with cyclic triaxial tests on ceramic beads-clay mixtures.

Keywords:
Sand-clay mixtures; Pore pressure build-up; Cyclic triaxial test; Cyclic torsional shear test; Pore pressure model

1. Introduction

Aggregate-clay mixtures are successfully used as the core of embankment dams or soil liner in waste disposal projects. These materials which were referred to as composite clays by Jafari and Shafiee [1], are usually broadly graded and encompass clay as the main body, and sand, gravel, cobble and even boulder as floating inclusions in the clay matrix. Moraine, which consists of unsorted materials of glacial origin, is a good example for this type of composite soils. Moraine has been used extensively in North America and northern countries as fill material for impervious cores in zoned embankment dams or for the main body of homogeneous dikes [2]. It has also served as relatively good quality foundation for water retaining structures. It is also a current practice to employ the mixture of high plastic clay with aggregates as impervious blankets in waste disposal projects [3-5].

Jafari and Shafiee [1] carried out a series of strain-controlled monotonic and cyclic triaxial tests on gravel-clay and sand-clay mixtures to investigate the effects of aggregate on the mechanical behavior of

the mixtures. Compression monotonic test results revealed that the angle of shearing resistance increased with aggregate content. It was also found that the presence of aggregates within a cohesive matrix led to formation of a heterogeneous field of density in the clayey part of the mixture. The strain-controlled undrained monotonic and cyclic tests also led to increase of Excess Pore Water Pressure (EPWP), when aggregate content was raised. Later experimental and numerical analyses also confirmed the heterogeneity formation in clay aggregate mixtures [6].

Despite the above mentioned studies, a review of the published literature reveals that experimental studies on aggregate-clay mixtures have mainly focused on shear strength parameters, particularly in compression loading. These studies report that shear strength either increases with aggregate content or remains constant until a limiting aggregate content, then increases as the aggregate content increases [1, 6] to explore all features of the mechanical behavior, there is a need to investigate pre- failure along with failure behavior of the mixtures subjected to various loading paths. The present study is an extension to the study performed by Jafari and Shafiee [1]. In this study, mixtures of isotropically/ anisotropically consolidated sand-lean clay were tested under strain- and stress-controlled loading conditions, making use of hollow cylinder torsional shear device along with triaxial device to comprehensively investigate EPWP in sand-clay mixtures. The results of monotonic compression and extension tests on the materials of this study, have been already published by Shafiee et al. [7]. It was shown that the angle of shearing resistance in sand-lean mixtures increases with sand content, and it is almost equal to the values obtained for sand-fat clay mixtures by Jafari and Shafiee [1], except at 60% sand content where sand-lean clay mixtures show slightly higher value for friction angle. From normalized shear strength data published by Shafiee et al. [7], it can be concluded that specimens consolidated under a confining stress of 100 kPa are overconsolidated, while specimens consolidated under confining stress of 300 kPa and higher are normally consolidated. Consequently, the experiments of this study were conducted on specimens consolidated under 100 kPa and 500 kPa confining pressure.

On the basis of the experiment results, a dissipated energy-based pore pressure model is developed, that considers the role of aggregate content as an independent parameter. The various loading paths followed herein, including the sudden or gradual rotation of principal axes in the triaxial and torsional shear devices respectively, has concluded to a generalized model capable of capturing EPWP in aggregate-clay mixtures. The model is then verified with a new set of data from cyclic triaxial tests on ceramic bead-clay mixtures.

2. Materials and Procedures

2.1. Tested Materials

Pure clay as the matrix and sand aggregates as inclusions were used in this study. The clay had a specific gravity (Gs) of 2.70, liquid limit (LL) of 42% and plasticity index (PI) of 18%. X-ray diffraction analysis revealed that the clay was mainly composed of kaolinite with some illite, montmorillonite, and quartz. The sand used in the study was retrieved from a riverbed and composed of subrounded particles with a specific gravity of 2.65. The aggregates used as sand material were passed through the 4.75 mm sieve and was retained on the 3.35 mm sieve, with minimum and maximum void ratios of 0.667 and 0.803, respectively. Gap graded gradation was considered for the aggregates to minimize the effect of particle size distribution of sand on the mechanical behavior of the mixture. Three mixtures were obtained by mixing 100, 60 and 40% of clay by volume with sand. A minimum of 40% clay content was considered since this is a limit value for materials used as cores in embankment dams. Figure (1) shows the materials used in this study.

2.2. Sample Preparation and Testing Procedure

The specimen preparation technique was chosen to model as precisely as possible the in situ condition of the core materials of embankment dams. All specimens, typically a cylinder 76 mm in height and 38 mm in diameter for triaxial tests, and a hollow cylinder 100 mm in height, and 100 and 50 mm in external and internal diameter respectively for torsional shear tests were prepared with a dry

(a) Sand Grains

(b) Clayey Soil

Figure 1. Materials used in this study.

density of 95% of the maximum dry density obtained from the standard compaction test method (ASTM D 698-12e2 [8]) and water content of 2% wet of optimum.

Table (1) presents the initial dry density and water content of the specimens. The specimens were saturated with a Skempton B-value in excess of 95%, and then isotropically consolidated under vertical effective stresses of 100 and 500 kPa. Following isotropic or anisotropic (K= initial vertical stress/initial horizontal stress = 2/3) consolidation, undrained cyclic triaxial and hollow cylinder torsional shear tests were carried out under strain- and stress-controlled condition. Tables (2) and (3) show the testing schedule in this study under strain- and stress-loading conditions respectively. The cyclic tests were continued until 50 cycles of loading. A loading frequency of 0.004 Hz for cyclic tests was chosen so that EPWP equalization throughout the specimen was ensured. Strain-controlled tests were performed under shear strain amplitudes (γ_c) of 0.75 and 1.5%, while stress-controlled tests were performed under cyclic stress ratios (CSR) of 0.11, 0.18 and 0.25. An advanced automated closed-loop digitally servo- controlled triaxial [9] and torsional shear [10] testing apparatus were used to conduct the tests. Figures (2a), and (2b) show sand-clay specimens after cyclic triaxial and torsional shear test respectively.

Table 1. Properties of the tested specimens.

Specimen	Initial Dry Density (kN/m^3)	Initial Water Content (%)
100% Clay	16.0	20.2
40% Sand - 60% Clay	18.5	13.0
60% Sand - 40% Clay	19.5	11.1

Table 2. Cyclic strain-controlled triaxial and torsional shear experiments conducted in this study.

Mixture	γ_c (%)	Anisotropic Consolidation Ratio, K	Effective Vertical Consolidation Stress (kPa)
100% Clay	0.75	1	100
	1.5	2/3	
	0.75	1	500
	1.5	2/3	
40% Sand – 60% Clay	0.75	1	100
	1.5	2/3	
	0.75	1	500
	1.5	2/3	
60% Sand – 40% Clay	0.75	1	100
	1.5	2/3	
	0.75	1	500
	1.5	2/3	

Table 3. Cyclic strain-controlled triaxial and torsional shear experiments conducted in this study.

Mixture	CSR	Anisotropic Consolidation Ratio, K	Effective Vertical Consolidation Stress (kPa)
100% Clay	0.11	1	100
	0.18		
	0.25		500
40% Sand-60% Clay	0.11	1	100
	0.18		
	0.25		500
60% Sand-40% Clay	0.11	1	100
	0.18		
	0.25		

(a) Triaxial (b) Torsional Shear

Figure 2. Sand-clay specimens after experiment.

3. Test Results and Discussions

3.1. Effect of Sand Content on the EPWP Build-up

Jafari and Shafiee [1] showed that EPWP in an undrained loading increases when aggregate content is raised under strain-controlled monotonic, and cyclic tests. This trend was also observed in this study, as depicted in Figure (3). The figure shows normalized residual pore water pressure, u_N^*, which is residual EPWP divided by initial vertical effective stress, under strain-controlled tests. Similar trend was observed in other strain-controlled tests of this study, which are not presented herein to observe brevity.

Figure (3) clearly shows that EPWP increases with sand content, under either cyclic triaxial or cyclic torsional shear (strain-controlled) tests. The increase in pore pressure with sand content can be attributed to the higher straining of the clayey part of the specimen, when sand content is raised [1].

Figure (4) shows the typical EPWP variation in sand-clay mixtures under stress-controlled loadings. It is observed that (on oppose to the strain-controlled tests) the EPWP decreases, when sand content is raised. This trend was observed in all the stress-controlled tests. This type of behavior can be explained by the aid of monotonic test results (conducted in this study) on pure clay and 60% sand - 40% clay mixture as shown in Figure (5).

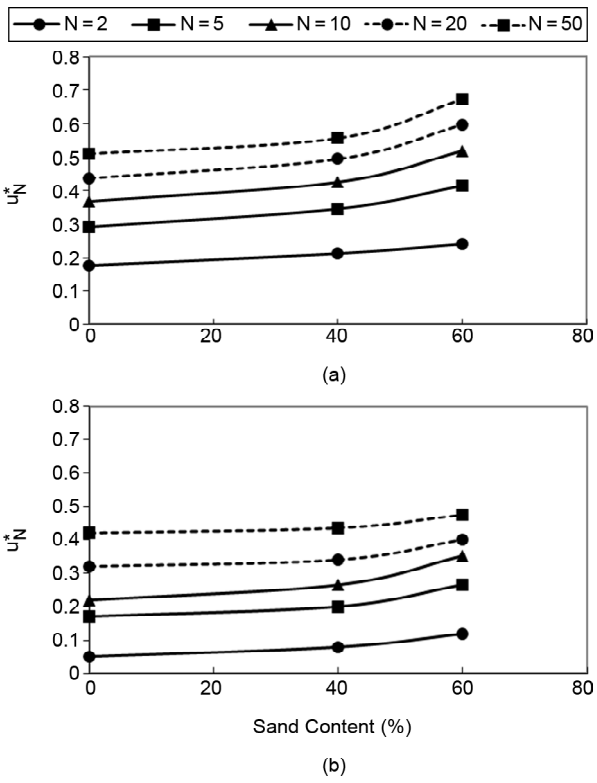

Figure 3. Normalized EPWP in strain-controlled tests, γ_c = 0.75%, initial confining stress = 100 kPa.

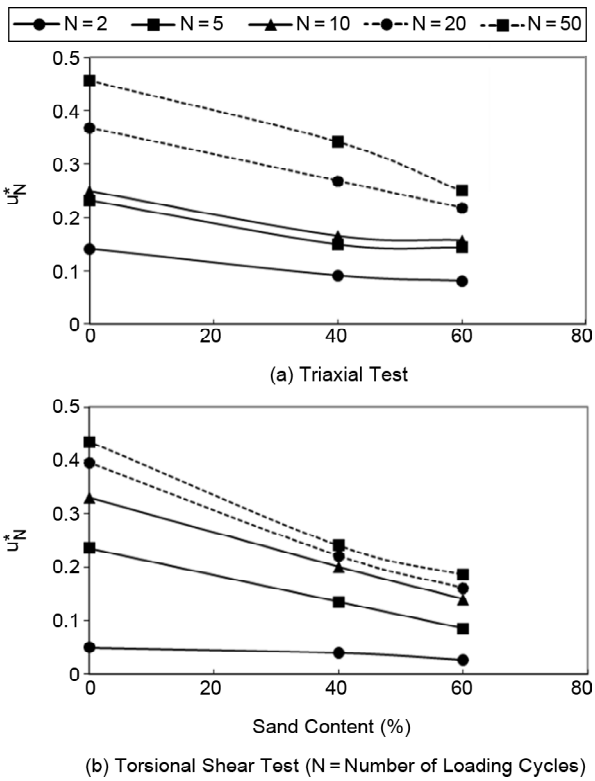

Figure 4. EPWP in stress-controlled tests, CSR = 0.18, initial confining stress = 100 kPa.

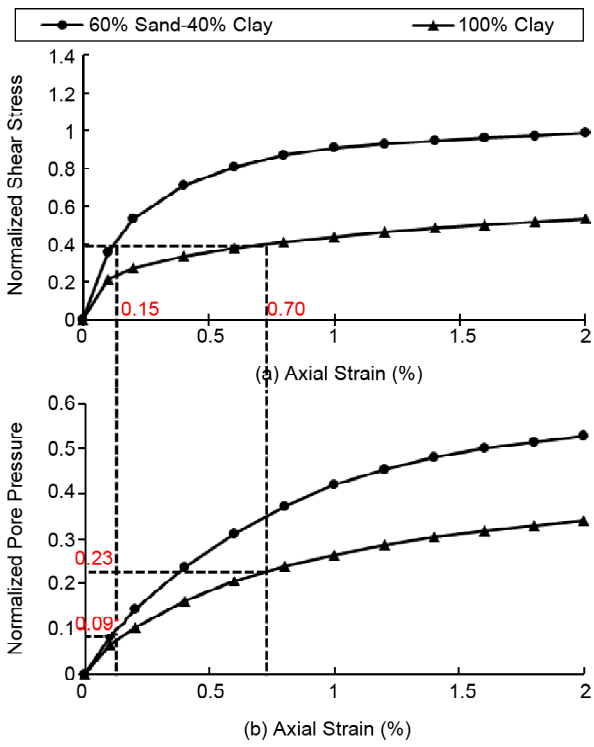

Figure 5. How excess pore pressure decreases with sand content in a stress-controlled test (initial confining stress= 100 kPa).

For example, under an identical stress ratio (=shear stress/initial confining stress) of 0.4, the amount of axial strain in sand-clay mixture, and pure clay is 0.15 and 0.70% respectively (Figure 5a). Consequently, under an axial strain of 0.15 and 0.70%, the amount of normalized pore pressure in sand-clay mixture and pure clay will be 0.09, and 0.23 respectively (Figure 5b). Thus, under an identical stress ratio, EPWP decreases with sand content.

Figure (6) compares sand-clay mixture behavior under strain- and stress-controlled triaxial tests. ($p' = \frac{\sigma_1' + 2\sigma_3'}{3}$, $q = \frac{\sigma_1' - \sigma_3'}{2}$, σ_1' and σ_3' = major and minor principal stresses).

As seen, in the strain-controlled tests, pore pressure increases, and significant degradation happens with number of cycles. In addition, stress path progressively moves toward the failure envelope. On the other hand, in the stress-controlled tests, pore pressure increases for a few cycles, with a minor degradation, after which the behavior is stabilized, in such a manner that almost no change in pore pressure and stiffness is observed. It seems that the higher magnitudes of strain in strain-controlled tests exceed the threshold shear strain for degradation [11], despite the lower magnitudes in stress-controlled tests which are within the threshold.

3.2. Effect of Rotation of Principal Stresses on EPWP

There is a fair amount of literature on the effect of principal stress rotation on shear strength, and EPWP of sands and clays in monotonic and cyclic tests. It has been shown that shear strength and

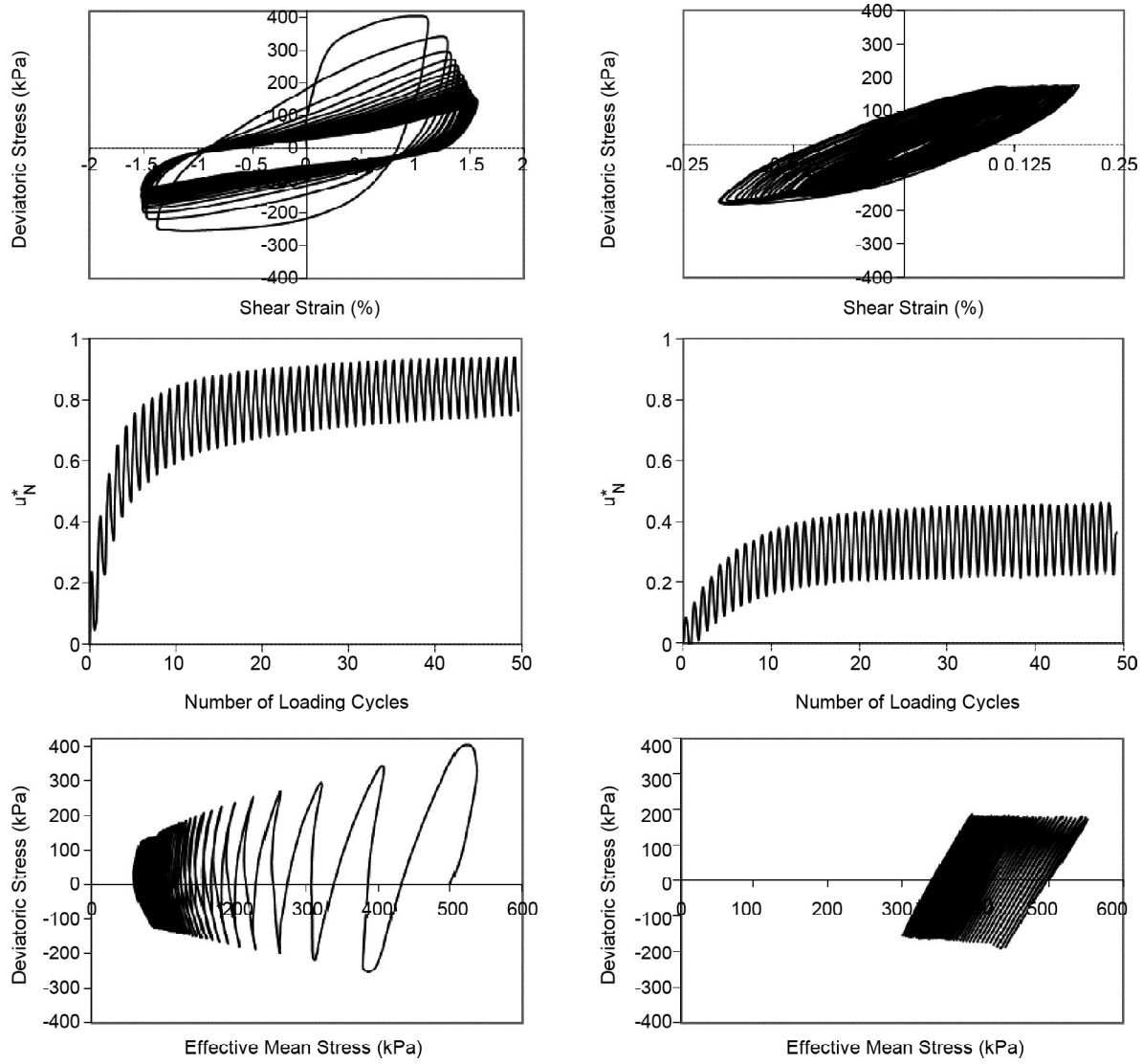

Figure 6. Cyclic triaxial strain-controlled (initial confining stress=500 kPa, and γ_c = 1.5%), and stress-controlled (initial confining stress = 500 kPa, CSR = 0.18) test results on 60% sand-40% clay specimens.

EPWP are affected by α (defined as the angle between major principal stress and vertical axis) [12-15]. With regard to cyclic tests, the effects of principal stress rotation on the cyclic resistance ratio (CRR) of liquefiable sands has been studied by comparing triaxial test results with those of simple shear device [16-18].

The materials tested in this study are highly anisotropic, because of the method of specimen preparation. Shafiee et al. [7] showed how the permeability of compacted aggregate-clay mixtures is affected by soil anisotropy. Consequently, EPWP pattern is expected to be highly affected by the principal stress rotation. In triaxial set-up sudden change of principal stress rotation during cyclic loading occurs, while under torsional shear condition continuous rotation of principal stress is captured. Figures (7a) and (7b) compare EPWP in triaxial tests versus torsional shear tests in stress-, and strain-controlled tests respectively.

It is mostly observed that higher residual EPWP is developed in triaxial with respect to torsional shear. As depicted in the figures, the variation of EPWP in triaxial tests is different from the torsional shear tests; while the latter is increasing smoothly, the former is fluctuating around its residual magnitude that is increasing.

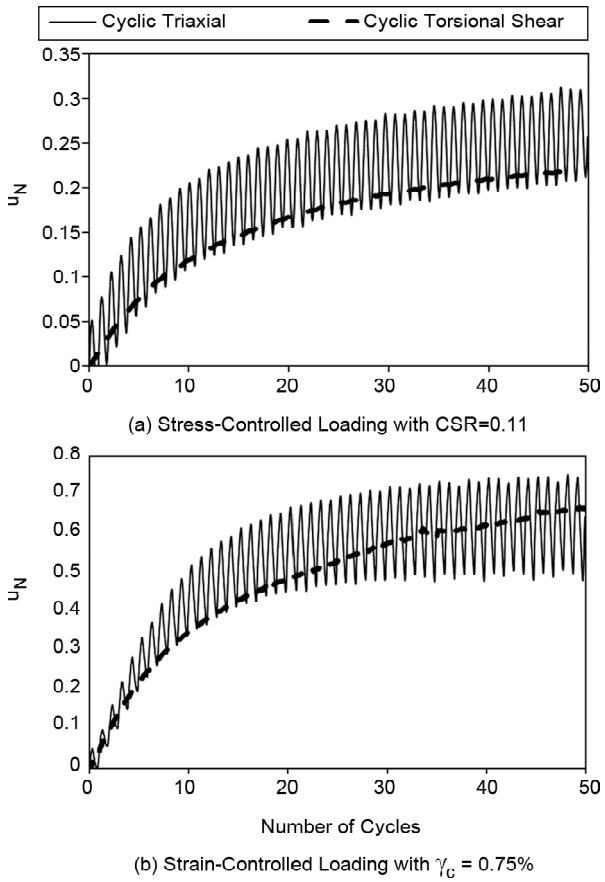

Figure 7. Variation of normalized EPWP (u_N) in cyclic triaxial and torsional shear test on 40% sand-60% clay specimen with 500 kPa initial confining pressure.

This inconsistency may be related to the different loading pattern of the testing apparatus and the relation of the mean confining pressure and EPWP in an elastic saturated soil [12]:

$$\Delta u = \frac{C_d}{C_d + nC_w}\Delta p \tag{1}$$

where:

$\Delta u = EPWP$

n = soil porosity

C_w = compressibility of the water

$C_d = \frac{3(1-2\mu)}{E}$ compressibility of the soil skeleton

Δp: variation of total mean confining pressure

The total mean confining pressure is fluctuating (Δp) in sinusoidal shape in the triaxial test, while is constant in the torsional shear test. Considering the EPWP is composed of an elastic and a plastic component, it is observed (Figure 7) that the fluctuation is the elastic component, while the residual increase is the plastic component. Consequently, the EPWP fluctuates in an elastic manner due to a portion of the Δp variation in triaxial test which is devoted to the elastic changes, but is constant in torsional test because of the zero Δp. However, the plastic increase of residual EPWP in both tests is due to the shearing of the soil beyond the degradation threshold.

3.3. Effect of Induced Anisotropy on EPWP

Some of the specimens in this study were consolidated anisotropically (K = 2/3), and tested in the triaxial device under strain-controlled conditions to investigate effect of induced anisotropy on the EPWP of sand-clay mixtures. Figures (8a) and (8b), for instance, presents the effect of induced anisotropy on EPWP in cycles 10 and 50 respectively, when shear strain amplitude is 0.75%. Similar to isotropically consolidated specimen, EPWP increases with sand content in anisotropically consolidated specimens. It is also observed that anisotropic

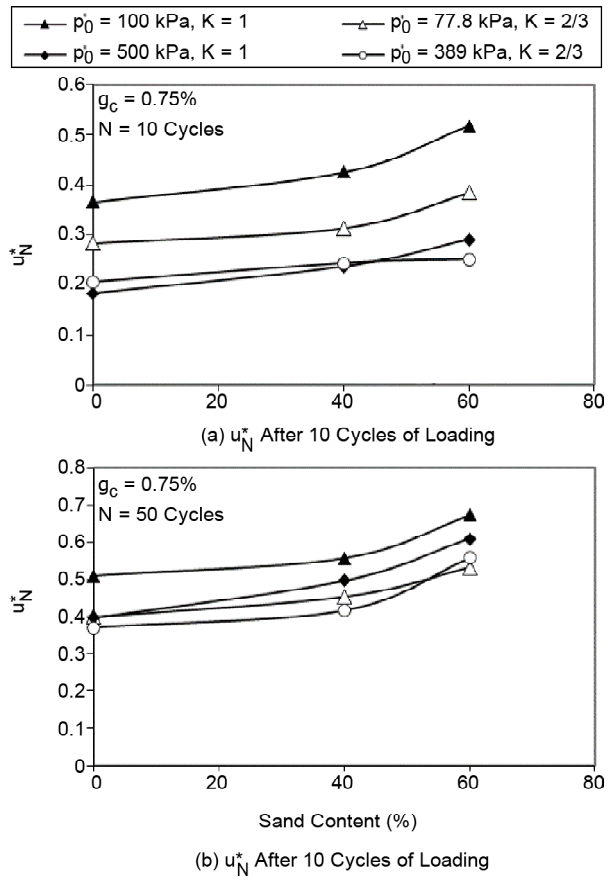

Figure 8. Variation of u^*_N with sand content in cyclic triaxial test on isotropically (K=1) or anisotropically (K=2/3) consolidated specimens.

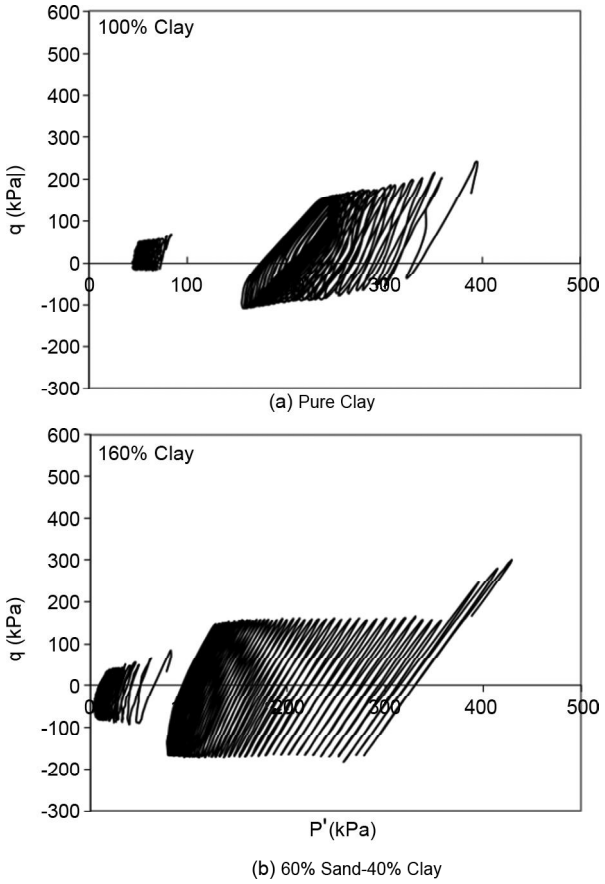

Figure 9. Variation of deviator stress with mean effective confining pressure in strain-controlled cyclic triaxial tests (γ_c = 0.75%) on anisotropically consolidated specimens.

consolidation would decrease EPWP in the sand-clay mixtures. Figure (9) compares stress path in q-p' space, for pure clay with 60% sand-40% clay mixture. Although stress path is asymmetry about p' = 0 axis in both cases at first cycle (Figure 9a), the effect of induced anisotropy diminishes after a few cycles in some cases, e.g. high confining pressure test on pure clay in 9a, and increases after a few cycles in some cases, e.g. low confining pressure test on mixed clay in 9b.

4. A Pore Pressure Model for Aggregate-Clay Mixtures

4.1. Energy Approach

Classical approaches for pore pressure models are mainly based on cyclic stress or strain amplitude [19-20]. However, results of the current study show that EPWP is highly dependent on loading path, and could be much different under stress- and strain-controlled loading. Here, EPWP is correlated to the dissipated energy, which considers the effects of both shear stress and shear strain variations during cyclic loading and has successful precedents in this regard [21]. Figure (10), for instance, shows variation of u^*_N in terms of normalized dissipated energy $(\Delta w / p'_o)$ for specimens tested in this study under cyclic triaxial conditions, with an initial effective mean confining stress of $p'_o = 500$ kPa.

Herein, Δw is dissipated energy per unit volume per cycle of loading, which is equal to the area of hysteretic loop in the shear stress-shear strain space. It is interesting to note that irrespective of loading path (stress- or stress-controlled test), and amplitude of loading, u^*_N exhibits strong relationship with dissipated energy.

The proposed pore pressure model is presented by:

$$u^*_N = u^*_N(\Delta w, \theta, p'_0, C) \tag{2}$$

in which:

Δw = dissipated energy in stress-strain space per unit volume (accumulated with cycles);

θ = Lode angle (the angle between stress state vector and σ'_1 axis on π-plane, $\theta = 0$, $\pi/3$ rad for

cyclic triaxial, and π/6 rad for torsional shear test);
p'_0 = initial mean effective stress
C = clay content ≤ 1.

Lode angle was included to account for the principle axis rotations in different loading paths. The parameter C also implicitly represents the role of aggregates in the predictions of the model.

To find the best model fitting the experimental data, different equations were examined utilizing least square approach. The experimental data included all the triaxial and torsional shear tests conducted in this study.

4.2. Fitting a Proper Model to the Test Results

To find the best fit for the available data, numerous trials finally concluded to the following equation ($R^2 = 0.75$):

$$u_N^* = f(\theta)\frac{A\left(\frac{\Delta w}{p'_0}\right)^{0.67}}{1+A\left(\frac{\Delta w}{p'_0}\right)^{0.67}} \quad (3)$$

in which

$$f(\theta) = 2.7\cos^2\theta - 4.1\cos\theta + 2.4 \quad (\theta = \text{Load Angle}) \quad (4)$$

$$A = 0.5BC^{-1.3} \quad (5)$$

$$\beta = \frac{\left(u_N^*\right)_{loop\ n} - \left(u_N^*\right)_{loop\ n-1}}{\left(\frac{\Delta w}{p'_0}\right)_{loop\ n} - \left(\frac{\Delta w}{p'_0}\right)_{loop\ n-1}} \quad (6)$$

The parameter β defines the rate of variation of u_N^* with $\frac{\Delta w}{p'_0}$ that is mainly dependent on the clayey part of the mixture. Value of β for the clay material used in this study fluctuated around 4. Figure (10) shows all the triaxial test results performed in this study versus the model under an initial confining stress of 500 kPa, as a sample of the general trend in all the cases. As observed, the model fits fairly well with the EPWP build-up in different tests on different mixtures.

4.3. Residual Analysis

Residuals (difference from measured to predicted values) of the u_N^* are plotted against $\frac{\Delta w}{p'_0}$ in Figure (11), which shows a relatively uniform distribution. The residual average and standard deviation (calculated as the square root of the average of the squared difference of residual from the mean residual) are also included in this figure, which has a horizontal trend. This means that $\frac{\Delta w}{p'_0}$ is a proper variable to describe u_N^*.

Figure (12) shows variation of the standard deviation of the u_N^* against clay content, distinguished by the apparatus type (triaxial or torsional shear). The overall trend does not show a special tendency in this

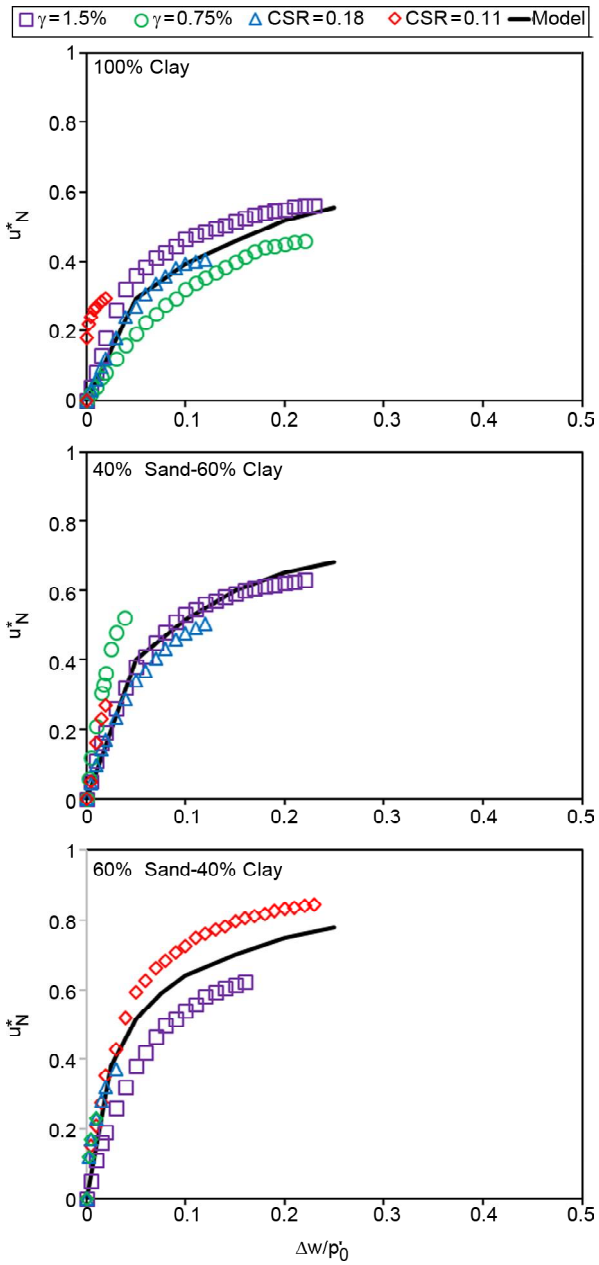

Figure 10. Correlation between excess pore pressure and dissipated energy in cyclic triaxial strain-/stress-controlled tests (initial confining pressure=500 kPa).

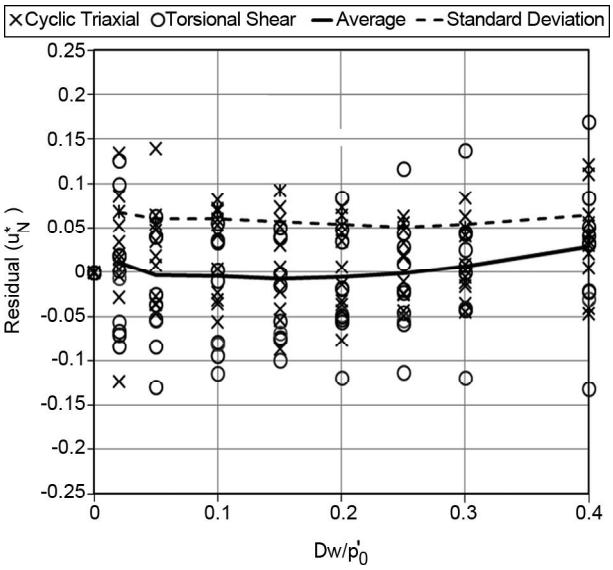

Figure 11. Residuals of the u^*_N calculated for all the experiments conducted in this study.

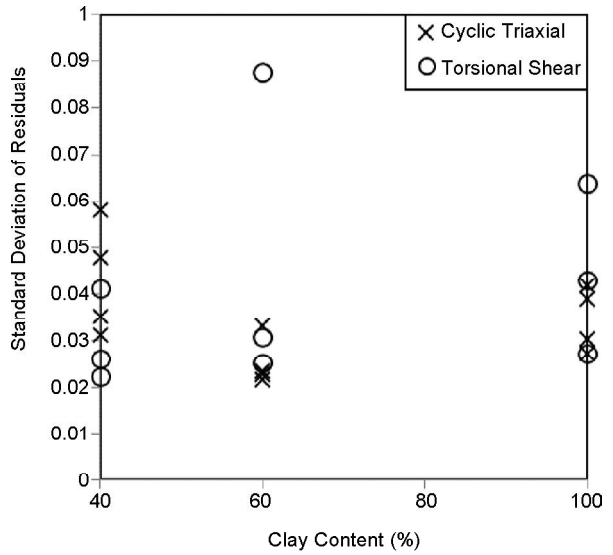

Figure 12. Standard deviation of the residuals of the u^*_N at different clay content.

regard, neglecting the only noticeably different magnitude at 60% clay content (which belongs to the specimen anisotropically consolidated to 100 kPa in torsional shear apparatus).

4.4. Evaluating the Proposed Model

To evaluate the proposed model, a different material and loading path was examined. A mixed specimen with 40% (volumetric) ceramic beads and 60% clay was tested in triaxial apparatus. The clay (G_s = 2.64, LL = 32, PI = 12) and ceramic inclusions (Diameter = 4 mm, and G_s = 3.73) were compacted in 10 layers to the 95% of maximum dry density of

Figure 13. The ceramic beads-clay material used for evaluation of the proposed model.

the material (which was 23 kN/m^3 with standard compaction method (ASTM D698-12e2)) at a water content 2% wet of optimum (woptimum = 8.1%). X-ray diffraction analysis revealed that the clay was mainly composed of quartz and kaolinite with some calcite. Figure (13) shows the wetted material before compaction. The specimen was then consolidated to 200 kPa effective confining stress isotropically, and subjected to 10 undrained cycles of variable confining pressure loading. The deviator stress and the confining pressure single amplitude was 80 kPa and 53 kPa respectively, at a frequency of 0.005 Hz. Figure (14) shows the variation of deviator stress, confining stress and EPWP with shear strain amplitude and loading cycles.

For this triaxial test, the input parameters of the Equation (3) are as follows:

$\theta = 0, \pi/3$ thus $f(\theta) = 1$; p'_0 = 200 kPa; C = 60 and β = 41

Based on the w measurement for different cycles, u^*_N was calculated (Figure 15). As evident, the proposed model predicts reasonably the EPWP variation in clay-aggregate mixtures without noticeable deviation with experimental measurements.

The important role of parameter β in Equation (3) is shown in Figure (16). Although the trend of EPWP build-up (Figure 16a), and deviator stress-axial strain relationship (Figure 16b) are dissimilar in two different tested clays, the choice of appropriate value of leads to a reasonable prediction of the pore water pressure trend in both specimens (Figure 15).

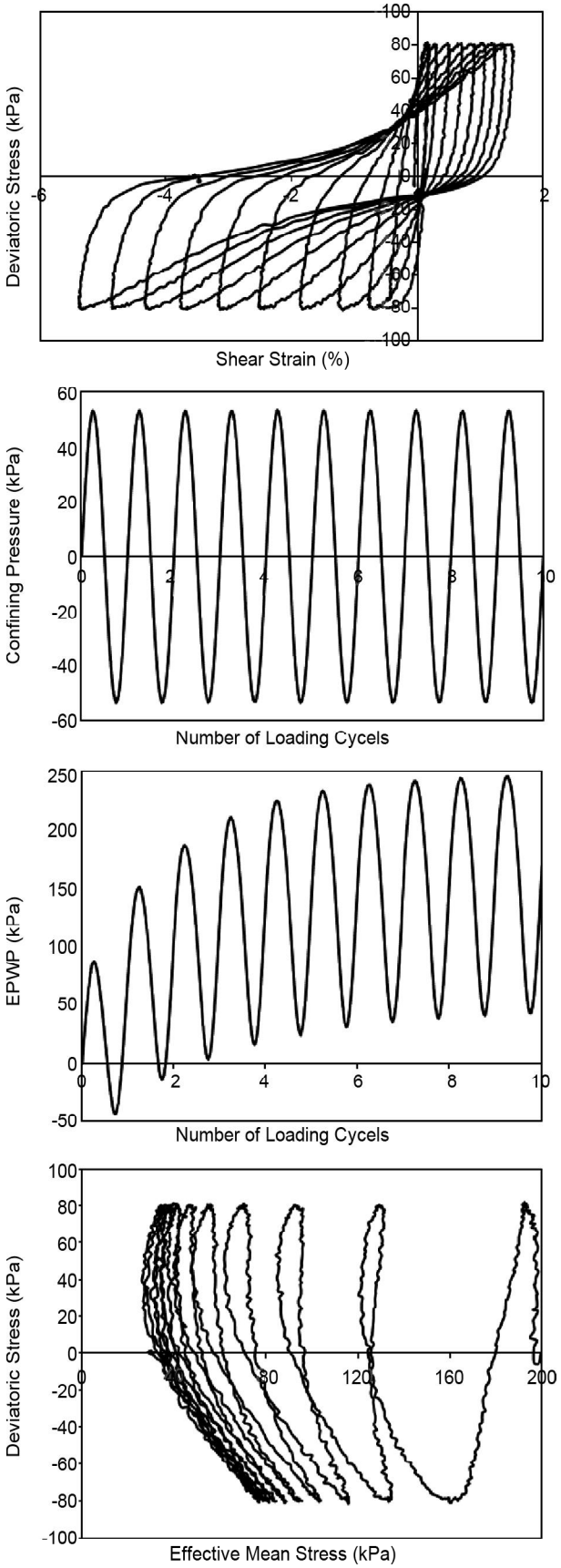

Figure 14. Validation cyclic triaxial test on 40% ceramic beads- 60% clay specimen.

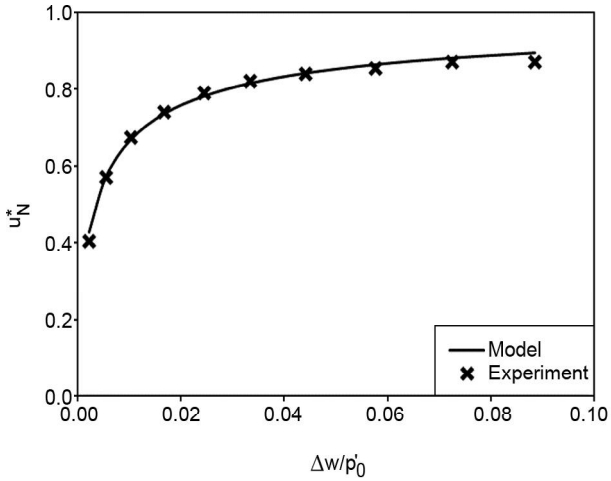

Figure 15. Predicted versus measured pore water pressure in 40% ceramic beads- 60% clay specimen.

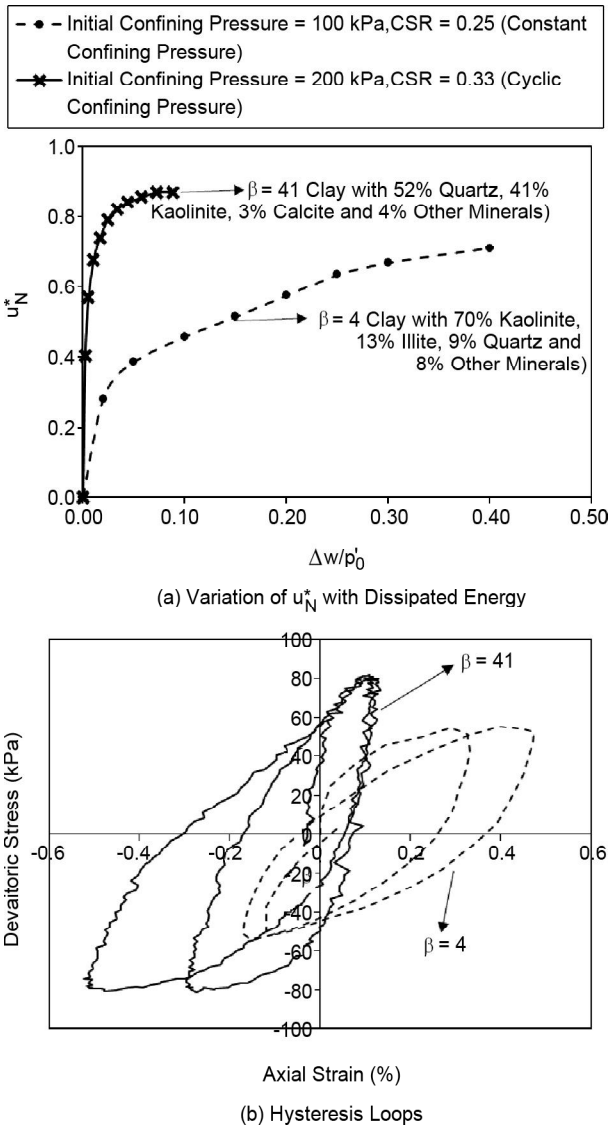

Figure **16.** Comparison of two different tested clays.

5. Conclusions

An experimental study using strain- and stress-controlled cyclic triaxial and torsional shear tests was performed on compacted mixtures of sand-clay to investigate pre-failure behavior of the mixtures in terms of EPWP variation in different loading conditions and mixture constituents. It was found that when sand content is raised, EPWP increases in cyclic strain-controlled tests, significant degradation occurs and stress path progressively moves toward the failure envelope. On the other hand, reverse trend is observed in cyclic stress-controlled tests, and EPWP decreases with sand content. In stress-controlled tests EPWP increases for a few cycles, with a minor degradation, after which the behavior is stabilized, in such a manner that almost no change in EPWP and stiffness is observed.

Effect of principle axes rotation was also examined by comparison of the triaxial and the torsional shear test results. It was mostly observed that higher residual EPWP is developed in triaxial with respect to torsional shear test.

Anisotropically consolidated specimens in strain-controlled tests were compared with isotropically consolidated ones, and the same trend of behavior with slight differences in initial hysteresis loops were observed. The magnitude of EPWP build-up in anisotropically consolidated specimens is lower than the isotropically consolidated ones. Effect of induced anisotropy in sand-clay mixtures diminishes after a few cycles of loading.

All the above-mentioned observations were taken into account to propose a dissipated-energy-based model, which can be successfully employed to predict the trend of EPWP build-up in sand-clay mixtures, irrespective of loading path. The model was verified through new set of the tests on ceramic beads-clay mixtures.

References

1. Jafari, M.K. and Shafiee, A. (2004) Mechanical behavior of compacted composite clays. *Canadian Geotechnical Journal*, **41**(6), 1152-1167. https://doi.org/10.1139/t04-062.
2. ICOLD (1989) Moraine as embankment and foundation material. *International Commission on Large Dams Bulletin*, **69**(13), Paris, France.
3. Demdoum, A., Gueddouda, M.K., and Goual, I. (2017) Effect of water and leachate on hydraulic behavior of compacted bentonite, calcareous sand and tuff mixtures for use as landfill liners. *Geotechnical and Geological Engineering*, **35**(6), 2677-2696, https://doi.org/10.1007/s10706-017-0270-4.
4. Meier, A.J. and Shackelford, C.D. (2017) Membrane behavior of compacted sand-bentonite mixture. *Canadian Geotechnical Journal*, **54**(9), 1284-1299. https://doi.org/10.1139/cgj-2016-0708.
5. Pandey, L.M.S. and Shukla, S.K. (2018) Effect of state of compaction on the electrical resistivity of sand-bentonite lining materials. *Journal of Applied Geophysics*, **155**, 208-216, https://doi.org/10.1016/j.jappgeo.2018.06.016.
6. Jalili, J., Jafari, M.K., Shafiee, A., Koseki, J., and Sato, T. (2012) An investigation on effect of inclusions on heterogeneity of stress, excess pore pressure and strain distribution in composite soils. *International Journal of Civil Engineering*, **10**(2), 124-138. http://ijce.iust.ac.ir/article-1-531-en.html.
7. Shafiee, A., Tavakoli, H.R., and Jafari, M.K. (2008) Undrained behavior of compacted sand-clay mixtures under monotonic loading paths. *Journal of Applied Sciences*, **8**(18), 3108-3118.
8. ASTM D698-12e2 (2012) *Standard Test Methods for Laboratory Compaction Characteristics of Soil Using Standard Effort (12 400 ft-lbf/ft3 (600 kN-m/m^3))*. ASTM International, West Conshohocken, PA, www.astm.org.10.1520/D0698-12E02.
9. Seiken (1998) *Technical Documentation of Combined Dynamic Triaxial and Resonant Column Test Apparatus*. Seiken Inc., Tokyo.
10. GCTS (2001) Geotechnical Consulting and Testing Systems. Tempe, Ariz. www.gcts.com.
11. Mortezaie, A. and Vucetic, M. (2016) Threshold shear strains for cyclic degradation and cyclic pore water pressure generation in two clays. *Journal of Geotechnical and Geoenvironmental Engineering*, **142**(5), 04016007. https://doi.org/10.1061/(ASCE)GT.1943-5606.0001461.

12. Lade, P.V. and Kirkgard, M.M. (2000) Effects of stress rotation and changes of b-values on cross-anisotropic behavior of natural, K0-consolidated soft clay. Soils and Foundations, **40**(6), 93-105, https://doi.org/10.3208/sandf.40.6_93.

13. Lin, H. and Penumadu, D. (2005) Experimental investigation on principal stress rotation in Kaolin clay. *Journal of Geotechnical and Geoenvironmental Engineering*, **131**(5), 633-642, https://doi.org/10.1061/(ASCE)1090-0241(2005)131:5(633).

14. Georgiannou, V.N., Konstadinou, M., and Triantafyllos, P. (2018) Sand behavior under stress states involving principal stress rotation. *Journal of Geotechnical and Geoenvironmental Engineering*, **144**(6), 04018028. https://doi.org/10.1061/(ASCE)GT.1943-5606.0001878.

15. Wang, Y., Gao, Y., Guo, L., and Yang, Z. (2018) Influence of intermediate principal stress and principal stress direction on drained behavior of natural soft clay. *International Journal of Geomechanics*, **18**(1), 04017128, https://doi.org/10.1061/(ASCE)GM.1943-5622.0001042.

16. Cavallaro, A. and Maugeri, M. (2004) Modelling of cyclic behaviour of a cohesive soil by shear torsional and triaxial tests. *Proceedings of the International Conference on Cyclic Behaviour of Soils and Liquefaction Phenomena*, Bochum, March.

17. Jefferies, M. and Been, K. (2015) *Soil Liquefaction: A Critical State Approach*. CRC Press. https://doi.org/10.1201/b19114.

18. Liu, J. and Chang, N.Y. (2017) *Liquefaction Resistant of Monterey No. 0/30 Sand in Cyclic Triaxial and Cyclic Hollow Cylinder Tests*. DES Tech Transactions on Materials Science and Engineering, ictim. 10.12783/dtmse/ictim2017/10044.

19. Finn, W.L. (2018) Evolution of geotechnical seismic response analysis from 1964 to 2015. *In Developments in Earthquake Geotechnics, Geological and Earthquake Engineering*, **43**, Springer, Cham. https://doi.org/10.1007/978-3-319-62069-5_2.

20. Dobry, R., El-Sekelly, W., and Abdoun, T. (2018) Calibration of non-linear effective stress code for seismic analysis of excess pore pressures and liquefaction in the free field. *Soil Dynamics and Earthquake Engineering*, **107**, 374-389. https://doi.org/10.1016/j.soildyn.2018.01.029.

21. Polito, C.P. and Moldenhauer, H.H. (2018) Energy dissipation and pore pressure generation in stress-and strain-controlled cyclic triaxial tests. *Geotechnical Testing Journal*, **42**(4), 1083-1089, https://doi.org/10.1520/GTJ20170437.